

1 **Loss of pelagic fish and zooplankton density associated with subglacial upwelling in high Arctic**
2 **estuaries may be mitigated by benthic habitat expansion following tidewater glacier retreat**

3 V. Gonzalez Triginer^{a,b}, A. Sen^a, M. Geoffroy^{b,c}, B. Damsgård^a

4 ^aDepartment of Arctic Biology, The University Centre in Svalbard, Longyearbyen, Norway

5 ^bFaculty of Biosciences, Fisheries and Economics, The Arctic University of Norway, Tromsø, Norway

6 ^cCentre for Fisheries Ecosystems Research, Fisheries and Marine Institute of Memorial University of
7 Newfoundland, St. John's, NL, Canada

8 Corresponding author: Victor Gonzalez Triginer; victor@unis.no

9

10

11

12

13

14

15

16

17

18

19

20

21

22 **Abstract**

23 Glacier fronts are hotspots of pelagic productivity due to upwelling of nutrient-rich water. As
24 tidewater glaciers retreat into land, this subglacial circulation will disappear and sedimentation from
25 terrestrial runoff will increase, leading to a decrease in pelagic productivity with a decline in the
26 abundance of fish and zooplankton. We used Billefjorden, a high Arctic fjord with a glacier recently
27 transitioned from sea- to land-terminating as a case study to identify spatial differences and small-
28 scale environmental drivers of density and vertical distribution of fish and zooplankton along a
29 gradient of glacier retreat (directly in front of the land-terminating glacier front, a river bay with
30 terrestrial input from land-terminating glaciers further inland and a location with minimal glacial
31 input). We developed a sustainable and efficient protocol to safely sample the glacier front and
32 shallow coastal areas using hydroacoustics and a remote autonomous vehicle combined with
33 oceanographic measurements and baited remote cameras. Over two years, pelagic density was
34 lowest at the now land-terminating glacier front and highest at the site with lowest terrestrial input.
35 Temperature, depth and turbidity explained less than 8% of the variation each. The site with the least
36 glacial input had the most heterogenous bottom habitat due to the presence of kelp forests, and the
37 richer demersal habitat likely contributed to the higher pelagic density. In shallow fjords and areas
38 with hard bottom substrate, it is expected that sea-ice and glacial retreat will promote macroalgal
39 settlement, and we suggest that macroalgal expansion may compensate the loss of tidewater glacier-
40 associated density of fish and zooplankton by the increase of benthic-driven density. Arctic pelagic
41 ecosystems could thus be more resilient to glacier retreat than initially thought, but this is highly
42 dependent on fjord topography, sedimentation rate and substrate type. Our developed protocol is an
43 efficient non-invasive method to survey shallow coastal areas and glacier fronts in the Arctic.

44 **Keywords**

45 Kelp forest, glaciers, fish, zooplankton, Svalbard, acoustics, climate change

46

47 **1. Introduction**

48 The impacts of global warming and climate change have been widely studied on offshore shelves and
49 in the open ocean, but knowledge gaps persist with respect to nearshore coastal areas and within
50 Arctic fjords and glacier fronts. The effects of retreating tidewater glaciers on fish distribution remain
51 particularly understudied, as they are areas under rapid change and very challenging to access and
52 monitor. The high abundance and biomass of zooplankton in glacier plumes suggest that glacier
53 fronts may serve as refugia for zooplankton-dependent food webs (Hop et al., 2023), and are
54 important feeding areas for key Arctic fish species such as polar cod (*Boreogadus saida*) (Lydersen et
55 al., 2014; Renaud et al., 2012). Upwelling from tidewater glaciers, caused by subglacial freshwater
56 discharge that rises to the surface, circulates nutrient-rich bottom waters and replenishes
57 zooplankton and juvenile fish to the surface waters, making these areas highly productive hotspots
58 for fish, marine mammals, and seabirds (Lydersen et al., 2014; Vonnahme et al., 2021). It has been
59 suggested that these areas provide refugia for Arctic species due to enhanced prey availability, as
60 access to other feeding areas such as the marginal ice zone becomes more energetically demanding
61 as the ice edge retreats (Hop et al., 2023; Varpe & Gabrielsen, 2022). As glaciers retreat, these
62 refugia are getting fewer and smaller but further research is needed to study how pelagic organisms
63 will react to these changes in littoral fjord areas.

64 Despite a shift from tidewater glaciers to land-terminating glaciers, significant amounts of nutrients
65 can nonetheless be brought into the sea through terrestrial runoff, groundwater discharge and
66 permafrost thawing (Holmes et al., 2008; Terhaar et al., 2021), which are increasing due to higher
67 precipitation and melting rates (Nowak et al., 2021). However, the associated high sediment and
68 freshwater input leads to higher stratification and light attenuation in the water column that inhibit
69 primary production at a local scale (Connolly et al., 2020; Halbach et al., 2019), and hence the
70 transition from tidewater to land-terminating glaciers is expected to negatively affect pelagic
71 productivity in Arctic fjords (Hopwood et al., 2020). Conversely, the retreat of tidewater glaciers and

72 sea ice is opening new areas where macroalgae can potentially settle and drive benthic primary
73 production (Assis et al., 2022; Krause-Jensen & Duarte, 2014), which may offset the loss of
74 production from tidewater glacier retreat and associated glacial upwelling. In deep fjords and coastal
75 areas where sediment runoff is increasing from land-terminating glaciers, macroalgal settlement may
76 be inhibited due to low light penetration and unsuitable settling substrate, but these interactions are
77 highly dependent on fjord topography and bottom substrate type. Macroalgae are ecosystem
78 engineers and provide important feeding and nursing sites for fish and benthic fauna (James &
79 Whitfield, 2023; Lippert et al., 2001), and a macroalgal expansion in the Arctic is expected to provide
80 opportunities for associated species (Włodarska-Kowalczyk et al., 2009). The interactions of glacial
81 discharge with the marine coastal ecosystem are complex, as there are several concomitant and
82 occasionally counteracting effects, and little empirical data exist on the transition from a rich
83 tidewater glacier front to a land-terminating glacier system, and particularly to what extent this will
84 affect fish and zooplankton communities in these areas.

85 Pelagic ecosystems at glacier fronts and shallow nearshore areas are challenging to study with
86 traditional sampling (e.g. gillnets, trawls) due to risks from drift ice, shallow rock formations and
87 difficulties operating vessels close to shore. Furthermore, these techniques have inherent biases such
88 as size and species selectivity and are invasive (e.g. bycatch and damage to the seafloor). For this
89 reason, coastal fish communities in Arctic fjords and their responses to glacier retreat are
90 understudied. Developing a methodology to efficiently and sustainably study fish and zooplankton
91 dynamics in these areas may provide a valuable link between the effects of glacier retreat on marine
92 biogeochemistry and primary production and changes in fish and zooplankton communities and
93 distribution. Alternative methods such as autonomous vehicles and hydroacoustics are emerging as a
94 sustainable and non-invasive method for ecological monitoring in the Arctic (e.g. Dunn et al., 2023;
95 Geoffroy et al., 2016). Though active acoustics are often used in conjunction with net sampling in
96 order to achieve higher taxonomic resolution and for ground truthing (Simmonds & MacLennan,

97 2005), scientific echosounders can be used as a standalone tool to record acoustic backscatter as a
98 proxy for density as well as vertical distribution patterns (Axenrot et al., 2004; Kaartvedt et al., 2009).

99 The aim of this study was to compare areas along a gradient of glacier retreat, from a very recently
100 transitioned glacier front from tidewater to land-terminating, a bay heavily affected by land-
101 terminating glaciers further inland to a site where glaciers have been absent for a long period of
102 time. Specifically, the density and vertical distribution of fish and zooplankton were compared
103 between the three study locations. Comparing different environmental conditions within a single
104 fjord provided a natural laboratory from which to measure the impacts from different physical
105 environmental parameters linked to glacier retreat and, ultimately, how it could apply to large-scale
106 modifications to the cryosphere. We hypothesized that land and glacial run-off at the river bay and
107 land-terminating glacier front, with high sedimentation rates and low light availability for primary
108 producers, leads to an area with low productivity and low biomass of zooplankton and fish.
109 Furthermore, we developed and present a protocol to study pelagic ecosystems in coastal and glacier
110 front habitats in the Arctic using a novel, cost-efficient and non-invasive technology.

111 2. Materials and methods

112 2.1 Study area

113 We conducted this study in Billefjorden, a high Arctic fjord located in Spitsbergen, Svalbard in
114 September 2021, August 2022 and August 2023. Billefjorden is characterized by a shallow sill (70 m
115 depth) at the fjord mouth which limits the inflow of Atlantic water from the West Spitsbergen
116 current that normally flows into the western fjords in Svalbard (Fig 1A). This allows Billefjorden to
117 stay colder than the surrounding fjords (Nilsen et al., 2008). Billefjorden has a heterogenous
118 coastscape with a large river bay and the glacier Nordenskiöldbreen located at the inner part of the
119 fjord (Fig 1B). This originally marine-terminating glacier has been retreating rapidly and the northern
120 side is now mostly land-terminating since 2017 (Kavan et al., 2023; Szczuciński et al., 2009).
121 Petuniabukta, located northwest from the glacier, gathers a high amount of sediment run-off from

122 the surrounding valleys and land-terminating glaciers through rivers (Láska et al., 2012) which creates
123 a river bay with a large tidal flat. Glacial freshwater input from rivers and the sediment plume of the
124 Nordenskiöldbreen glacier decrease with distance from both the river bay and the
125 Nordenskiöldbreen glacier bay, and becomes minimal in the middle of the fjord, where the glacier
126 front retreated 11,000 years ago (Baeten et al., 2010). This allows for a natural laboratory and the
127 systematic comparison between the recently land-terminating glacier site (GLA), the river bay (RIV)
128 with inland glacier-derived river input, and a site with minimal glacial input that can be considered
129 practically as a control site for glacial influence (CON) (Fig 1B).

130 2.2 Survey design

131 At each of the three stations (RIV, GLA and CON), pelagic backscatter, a proxy for density of pelagic
132 organisms, was measured via active acoustic mapping with a downward facing BioSonics DTX
133 scientific split-beam echosounder (BioSonics, Seattle, USA) mounted to the rear of an Uncrewed
134 Surface Vehicle (USV). Hydroacoustics is commonly used as a method to study fish and zooplankton,
135 as these organisms scatter sound due to the contrast between their morphological properties (e.g.
136 gas-filled structures and hard exoskeletons) and the surrounding water (Simmonds & MacLennan,
137 2005; Stanton et al., 1996). Metrics of acoustic backscatter were recorded to quantify abundance and
138 density of fish and zooplankton in the water column. We used an Otter USV (Maritime Robotics,
139 Trondheim, Norway), an electric 200 x 108 x 106 cm vehicle which was controlled remotely via
140 broadband communication radio (Direct link 5150 – 5875 MHz) from a nearby ship. The echosounder
141 was used at an operating frequency of 200 kHz, which is commonly used to detect and study fish and
142 zooplankton (Simmonds & MacLennan, 2005), a ping rate of 5 Hz and pulse duration of 0.4 ms.
143 Georeferencing of the acoustic data was done through the USV's internal Global Navigation Satellite
144 System (GNSS). Hydroacoustic mapping was done by running the USV in transects at an approximate
145 speed of 3 knots perpendicular to the shoreline twice, in August 2022 and August 2023. The middle
146 points of the transects were between 200 m and 800 m away from shore and with an average of 30

147 m water depth at all sites, with all stations covering the minimum range of 24 m to 42 m depth. In
148 2022, the transects were 17 minutes long covering an area of 2.8 ha and were done 6 times at each
149 station (Supplementary fig 1). In 2023, the sampling area was increased for each station to 8.5 ha and
150 45 minutes long transects by increasing the number of transect lines and were conducted 2 times.
151 Each time the transects were run is considered a replicate (6 replicates in 2022 and 2 replicates in
152 2023).

153 To characterize the physical environment, oceanographic data were collected via a Valeport SWiFT
154 CTDplus with Turbidity (Valeport Ltd., Totnes, UK). CTD water column deployments were conducted
155 from the ship to record temperature (degrees Celsius), salinity and turbidity (nephelometric turbidity
156 units; ntu) before the acoustic surveys. CTD profiles were taken for the entire water column (surface
157 down to bottom depth) at the three stations in both years. The CTD deployments were taken at
158 approximately 200 m from the center of the acoustic transects. These data were recorded to broadly
159 characterize and compare the different study sites, as a high-resolution description of the
160 oceanography of these areas would require a more comprehensive survey. Temperature and salinity
161 profiles were also used to calculate the speed of sound and coefficients of absorption to calibrate the
162 acoustic data.

163 To document the benthic habitat and bottom substrate type, baited remote underwater video
164 deployments (BRUV) were done once at each of the stations in September 2021. The BRUV rig
165 consisted of a metal frame with a GoPro camera and a 1 m- long arm holding a mesh bag with 1 kg of
166 polar cod (*Boreogadus saida*) as bait. The BRUV was lowered to the bottom at a depth of 10 m and
167 recorded video for 1 hour at each station. The maximum number of individuals observed at the same
168 time at any one time on the entire video (MaxN) was used as a measure of relative abundance of
169 taxa, which is commonly used in BRUV analyses to avoid double-counting (Osgood et al., 2019).

170 **2.3 Hydroacoustic analyses**

171 All raw acoustic files were extracted from the USV system and merged to create a single file for each
172 station using Visual Acquisition v6.4.1.12747 (BioSonics, Seattle, USA). Acoustic data were
173 subsequently processed in Echoview 13.1.121 (Echoview Software Pty Ltd, Tasmania, Australia). For
174 each station, the file was scrutinized for noise and a bottom line was set by using the “Best bottom
175 candidate” algorithm. A smoothing filter was applied to correct for benthic fish merging with the
176 bottom signal, and very minor manual editing was done to correct for gaps in the bottom line when
177 the signal momentarily dropped below the threshold. An exclusion line was added at a fixed depth of
178 5 m to exclude near field region noise close to the transducer, as well as a line 1 m above the bottom
179 to exclude bottom noise, and the analyses were limited to the water column in between the
180 exclusion lines.

181 To study variability in pelagic density between replicates for each station, each replicate of the 2022
182 data were then divided in 1-minute long echointegration cells, for a total of 17 grids (as each run was
183 17 minutes long), and the integrated volume backscattering strength (Sv in the logarithmic form dB),
184 center of mass (in m) and inertia (in m²) for each cell were exported for further processing and
185 analyses in the R statistical software v4.1.2 (R Core Team, 2021). Volume backscattering strength (Sv)
186 is a proxy for the density of organisms, center of mass identifies the average backscattering depth in
187 the water column, and inertia is a measure of the spatial dispersion of scatterers around their center
188 of mass (Urmy et al., 2012). A low inertia indicates tightly packed scatterers, while a high inertia
189 indicates a larger spread.

190 The acoustic data was also exported as one file per replicate and the center of mass, inertia and Sv in
191 the logarithmic form (dB) were plotted to visualize dissimilarities between the stations (CON, RIV and
192 GLA) and years (2022 and 2023) in terms of their acoustic properties. To assess potential
193 relationships between pelagic biomass and oceanographic conditions among stations and years, the
194 acoustic and CTD datasets were structured in 1 m depth bins and the data merged by depth bin
195 (CON: 5 m – 43 m, GLA: 5 m – 46 m, RIV: 5 m – 37 m in 2022; CON: 5 m – 47 m, GLA: 5 m – 50 m, RIV:

196 5 m – 34 m in 2023). A correlation matrix was done and a permutational multivariate analysis of
197 variance (PERMANOVA) was conducted with Sv mean in the linear form (m^2/m^3) as the response
198 variable and temperature, turbidity, depth, year and station as explanatory variables. A separate
199 PERMANOVA was conducted with salinity instead of temperature as explanatory variable to avoid
200 multicollinearity between temperature and salinity (Supplementary fig 2). As the top 5 m layer of the
201 acoustic data had to be excluded due to near field noise, the analyses of the environmental data are
202 therefore not including the top layer of the water column. As the CTD water profiles and acoustic
203 transects had slightly different depth ranges, these analyses were performed only for the depth bins
204 where both acoustic and CTD data were available. The “dplyr” and “vegan” packages were used in
205 Rstudio to arrange and export the data as tables and to conduct the NMDS and PERMANOVA
206 analyses. ArcGIS Pro v.3.1 was used to map the locations of the sampling stations.

207 3. Results

208 3.1 CTD water column profiles

209 The bottom depth at the CTD sampling stations was 37.6 m and 34 m at the RIV station, 46.4 m and
210 50.6 m at the GLA station and 53.7 m and 54.4 m at the CON station in 2022 and 2023, respectively
211 (Table 1, Figure 2). The ranges of temperature (max temperature – min temperature) were highest at
212 the CON station with 10 °C, and lowest at the RIV station with 6.5 °C. Salinity ranges were highest at
213 the GLA station with 18.2 psu, and lowest at the CON station with 3.8 psu. Turbidity ranges were
214 highest at the GLA station with 102.5 ntu and lowest at the CON station with 2.5 ntu. The GLA station
215 showed the highest surface turbidity and lowest surface salinity in both years, indicating a highly
216 stratified surface water layer.

217 3.2 Pelagic density and vertical distribution

218 The bottom depths at the study sites during the acoustic mapping surveys ranged from 5 to 56 m
219 (Table 2). The RIV station had a flat and homogenous bottom topography, while the GLA station had
220 an irregular bottom with steep cliffs and the CON station showed a gradual slope (Fig 3).

221 In 2022, Sv values and standard deviation were two orders of magnitude higher at the CON station
222 than at the other two stations, indicating higher pelagic density and higher variability at this station
223 (Fig 4, Table 2). Several large pelagic aggregations producing a strong backscatter were observed in
224 the echogram and are likely the cause of the high variation in Sv values at the CON station (e.g. Fig 3,
225 right panel). Pelagic density was similar between the glacier and river stations. The glacier station
226 had the deepest center of mass at 24.7 m and highest inertia at 147.2 m², which was reflected by a
227 deep and dispersed scattering layer in the echograms from 15 m depth down to the bottom.

228 In 2023, the GLA and RIV stations displayed higher pelagic density than the previous year, with an
229 increase of one and two orders of magnitude respectively. The RIV and CON stations showed an
230 increase in center of mass which could be linked to several strong scattering aggregations deeper in
231 the water column at both stations (Fig 3). The GLA station showed the lowest backscatter with one
232 order of magnitude lower than the CON and RIV stations, and the highest inertia at 169.7 m²
233 reflecting a disperse scattering layer. Despite the interannual differences mentioned above, the CON
234 station consistently reflected the highest pelagic density (Fig 4).

235 The variability of the logarithmic Sv values between replicates was higher at the CON station, with
236 values ranging from -80 dB to -45 dB (Fig 5). At the GLA and RIV stations, Sv values ranged between -
237 90 dB and -75 dB and between -87 dB and -75 dB respectively.

238 **3.3 Acoustic backscatter and physical oceanography**

239 The correlation matrix showed a high correlation between temperature and salinity (-0.88), and
240 hence these variables were analyzed in separate PERMANOVAs. The PERMANOVA analysis revealed
241 weak but significant effects ($p < 0.05$) of temperature turbidity and depth as well as station and year
242 on the variation of pelagic density (Table 3). Of the CTD measurements, turbidity showed the
243 strongest effect with an F value of 27.89, while year showed the strongest effect overall with an F
244 value of 59.74. Temperature had the weakest effect on pelagic density with an F value of 4.87.

245 However, temperature and turbidity only explained $\leq 8\%$ of the variation in pelagic backscatter each,

246 indicating the importance of other drivers. Salinity showed no significant effect on pelagic density
247 with an F value of 1.37 and $p > 0.05$ (Table 4).

248 **3.4 BRUV**

249 The BRUV footage revealed an abundance of fish, crabs and large zooplankton at the CON station, in
250 which dense kelp beds could also be observed (Fig 6A). The visibility at the glacier and river stations
251 was low, but the BRUV showed a more homogenous landscape at these stations compared to the
252 CON station, with almost no macroalgae. Three unidentified fish were observed at the glacier station
253 while no organisms were observed at the river station (Table 5).

254 **4. Discussion**

255 **4.1 Links between cryosphere changes and pelagic density and distribution**

256 Tidewater glacier fronts are highly productive pelagic environments due to subglacial nutrient
257 circulation, but as these glaciers retreat onto land the upwelling of nutrients disappears. In coastal
258 areas with high influence of land-terminating glaciers either directly in front or due to river runoff
259 from inland glaciers, high sedimentation rates and subsequent low light availability would lead to less
260 productive pelagic ecosystems (Hopwood et al., 2020). Among our three study sites along a gradient
261 of glacier influence, the acoustic data consistently showed higher pelagic density at the CON site with
262 the lowest glacial influence, and the higher standard deviation and wider range of Sv values between
263 the replicates at this site indicate a more productive and dynamic pelagic system at this site than at
264 the GLA and RIV stations with higher glacial influence. Although it is difficult to identify the organisms
265 that compose the scattering structures with a single frequency acoustic system, the large and strong
266 scattering aggregations visible in the echogram at the CON station and large variability of Sv values
267 within grids likely indicate large fish schools. In the absence of data indicating large fish schools, the
268 pelagic density was consistently low which suggests these fish schools and scattering aggregations
269 with high Sv values drive the high pelagic density at the CON station. The echograms and acoustic
270 analyses showed the large strong scattering aggregations to be linked to the bottom, which was

271 consistent with the BRUV footage in which numerous crabs, benthic fish and mysid shrimp appeared
272 next to the bait bag and indicated a rich demersal habitat and high densities of organisms on or near
273 the seafloor.

274 In contrast, the two glacier influenced stations (RIV and GLA) showed a generally lower pelagic
275 density over the water column, albeit with several small fish schools causing a higher acoustic
276 backscatter at the river station in 2023. While the acoustic data showed fish schools associated to
277 the bottom at the CON station, the scattering aggregations were dispersed across the water column
278 at the river and glacier sites. One explanation for this difference could be due to variation in
279 topography between the study sites. For instance, the steep cliffs at the glacier front at the GLA
280 station likely contribute to a dispersed scattering layer and the observed higher inertia. Conversely,
281 the flatter bottom at the river site may lead to a concentrated scattering layer. Nonetheless, the
282 echograms show distinct patterns in that, when fish schools are present, these aggregations are
283 small and dispersed over the water column at the river and glacier stations, while they are large and
284 associated to the bottom at the CON station as is shown by the higher Sv values and lower inertia.
285 The similarities in pelagic density and distribution between the glacier and river stations, particularly
286 in 2022, may be linked to the parallels in environmental conditions between these two sites, namely
287 the high sediment input from rivers and glaciers, which hinders the settling of benthic primary
288 producers and favors a pelagic-associated ecosystem (Hop et al., 2023). Furthermore, the depth
289 range of the river station was deeper than the depth distribution of macroalgae in Svalbard (Düsedau
290 et al., 2024), but macroalgal growth would not be expected in a river bay with high sediment load.
291 Conversely, the depth ranges at the GLA and CON stations covered shallower ranges (from 5 m and 7
292 m depth respectively) where macroalgae could be present. Similarly to the river bay, at the glacier
293 front, albeit land-terminating, there is a high sediment input as shown by the high turbidity values
294 and by the BRUV footage and hence the low light regime may hinder macroalgal growth. At the CON
295 station, however, the low glacial input, low turbidity and rocky substrate facilitates macroalgal
296 settlement as seen on the BRUV. These differences in light regime leading to a richer benthic and

297 demersal habitat at the CON station may explain the differences in pelagic density and distribution
298 between the sites.

299 The ranges in the oceanographic measurements indicated that salinity and turbidity values fluctuate
300 more at the RIV and GLA stations compared to the CON station, particularly in the surface layer, likely
301 due to freshwater and sediment input from the rivers and glacier. Furthermore, the high values of
302 turbidity observed at the glacier station may be linked to sediments being brought by currents from
303 the nearby tidewater glacier plume. The analysis of the relationship between pelagic biomass and
304 oceanographic measurements showed only weak statistically significant effects of temperature,
305 depth and turbidity on the acoustic backscattering strength, and no significant effect of salinity. It
306 should be noted that due to removing the top 5 m of the water column in the acoustic analyses to
307 eliminate near field noise, this shallow layer was also omitted from the CTD data when merging the
308 datasets and therefore is not included in the statistical analyses. As the water column CTD profiles
309 showed, the highest variability in the physical oceanography was in the top layer, likely due to the
310 sediment plumes from the river bay and glacier. Therefore, in the top 5 m environmental conditions
311 may be more important than at deeper depths, as high variations in salinity and temperature can
312 drive the abundance and movement dynamics of fish and zooplankton. Differences in these
313 environmental factors between the stations can drive the patterns of pelagic density and distribution
314 deeper in the water column (e.g. high surface turbidity at the glacier front reduces light availability
315 and may alter the vertical distribution of fish and zooplankton). However, as temperature, depth,
316 salinity and turbidity explained little of the variation, other factors must thus have a major role to
317 drive ecosystem dynamics. As seen on the BRUV footage, there was a rich benthic and demersal
318 ecosystem at the CON station, characterized by dense kelp beds, at least in the shallow areas that are
319 within the depth distribution of kelp in Svalbard. Conversely, little macroalgal coverage was observed
320 at the river and glacier stations, likely due to the high sediment input, low light availability and soft
321 bottom substrate. The BRUV was deployed in 2021 and therefore not concurrent with the acoustic
322 study, and hence there are limitations in comparing these data, but the underwater footage provides

323 a snapshot of the benthic habitat and substrate type, which is likely an important driver for pelagic
324 density at the deeper parts of the stations. The high sedimentation at the river and glacier sites was
325 visible in the BRUV footage, while there was more light availability and hard substrate at the site with
326 less terrestrial runoff.

327 In shallow areas with hard bottom, low sedimentation input and little mechanical disturbance,
328 macroalgal growth can be stimulated and lead to a high associated biomass of organisms that feed
329 on the algae or use them as shelter or nursery grounds (James & Whitfield, 2023; Lippert et al., 2001;
330 Teagle et al., 2017). Glacier and sea-ice retreat open up new areas where marine organisms can
331 settle, and previous studies have shown that macroalgae are expanding northward (Assis et al., 2022;
332 Krause-Jensen & Duarte, 2014) and settling at retreating glacier fronts (Deregibus et al., 2023;
333 Gonzalez Triginer et al., 2024). In shallow coastal areas, these demersal habitats can also benefit
334 pelagic fish and zooplankton, which may explain why both the demersal habitat richness and pelagic
335 density were consistently higher at the CON site. The effects of the expansion of these habitats in the
336 Arctic on fjord ecosystem dynamics are complex, and conducting similar studies in other areas would
337 aid in understanding their potential in mitigating the loss of pelagic productivity due to glacial
338 retreat. Our results are consistent with the literature in showing that areas influenced by land-
339 terminating glaciers and rivers may be linked to lower density of fish and zooplankton compared to
340 areas without the influence of terrestrial runoff (Hopwood et al., 2020). In our study, the site with
341 the highest recorded pelagic density had the lowest influence from rivers and glaciers, which
342 potentially allowed for settlement and growth of macroalgae. It has been suggested that an
343 enhanced demersal habitat expanding into areas previously covered by tidewater glaciers might be
344 beneficial to both benthic and pelagic organisms, at least in shallow ecosystems. A recent study in
345 inner Billefjorden recorded macroalgal settlement in areas that were covered by the glacier until very
346 recently, while there was virtually no macroalgal coverage at the river bays (Gonzalez Triginer et al.,
347 2024). However, there is limited data on the potential of macroalgal expansion to offset the loss of
348 productivity driven by subglacial upwelling in high Arctic fjords, and it is likely closely linked to fjord

349 topography and land runoff in coastal fjord areas, and hence highly vary between fjord systems.
350 More research is needed to further study the expansion of rich demersal habitats following glacial
351 retreat and their role in ecosystem dynamics and fjord productivity in the Arctic.

352 **4.2 The potential of autonomous hydroacoustic surveys in coastal areas**

353 The acoustic properties of the water column in shallow coastal areas can be highly dynamic and
354 complex, and therefore both echogram visualization and data analyses need to be taken into
355 consideration when interpreting the results. Moreover, complementing the acoustic data with
356 underwater video and oceanographic measurements further aids in understanding the complexity of
357 a spatial comparison of pelagic distribution. As a measure of the average backscatter depth in the
358 water column, the center of mass metric is sensitive to being skewed by outliers in the data such as
359 fish aggregations. Inertia is a measure of dispersion or spread of scatterers, and it considers both the
360 squared distances from the center of mass and their Sv values (Urmy et al., 2012). Therefore, inertia
361 is less sensitive to outliers and can lead to a representative measure of pelagic dispersion, and a
362 combination of center of mass and inertia are a more robust measure of the location and dispersion
363 of the pelagic scattering layer.

364 The efficiency of hydroacoustics to map and assess pelagic biomass in the Arctic has been shown in
365 multiple studies (e.g. Benoit et al., 2008; Geoffroy et al., 2019; Kaartvedt et al., 2009), but validation
366 of acoustic data is still critical to identifying species and functional groups. Validation of such data is
367 often done by trawl surveys (Geoffroy et al., 2019), but when working in shallow littoral areas it is
368 often not possible to trawl, and alternative validation methods are very limited and often biased,
369 especially in muddy and shallow glacier front areas.

370 Acoustic surveys have been done in the high Arctic in the past to map macroalgae coverage (Kruss et
371 al., 2017; Wiktor et al., 2022), and such methodology can be adapted to study the pelagic
372 environment in these areas. The inaccessibility of glacier fronts and remote areas in the high Arctic
373 makes it challenging to use traditional methods for marine sampling in coastal areas, and

374 autonomous hydroacoustic and remote sensing techniques can be used to safely and efficiently
375 study these sites, which are undergoing large changes due to climate shifts. The use of such novel
376 methodology allowed for sampling very close to the glacier front, which would not be possible from a
377 ship. This allowed to gain new insight on glacier fronts, which, as boundaries between the cryosphere
378 and the marine ecosystem, are key areas to understanding the effects of climate change on marine
379 biological processes. As rich benthic habitats such as kelp forests expand following glacier retreat,
380 littoral fjord areas in the high Arctic may be more resilient to loss of biomass and biodiversity than
381 previously thought.

382 **Acknowledgements**

383 We would like to thank Kathy Dunlop and the Institute of Marine Research for the loan of the BRUV
384 and for helping with the setup. We also thank the technical staff at the University Centre in Svalbard
385 for their support during long hours of fieldwork. We would like to thank the reviewers for their
386 valuable input which helped to improve our manuscript.

387 **Competing interests**

388 The authors declare there are no competing interests.

389 **Funding**

390 This study was financed through the FACE-IT project which has received funding from the European
391 Union's Horizon 2020 research and innovation programme under grant agreement No. 869154. MG
392 acknowledges funding from the Canadian Natural Sciences and Engineering Research Council
393 (NSERC) Discovery Grant program, and RCN-funded projects Deep Impact (#300333) and Opkrop
394 (#343352).

395 **Data availability**

396 The CTD profile datasets are publicly available at <https://doi.org/10.5281/zenodo.13323435>. The
 397 acoustic data generated and analyzed during this study fall under confidentiality regulations of the
 398 Norwegian Mapping Authority.

399

400 **References**

- 401 Assis, J., Serrão, E. A., Duarte, C. M., Fragkopoulou, E., & Krause-Jensen, D. (2022). Major Expansion
 402 of Marine Forests in a Warmer Arctic. *Frontiers in Marine Science*, *9*, 850368.
 403 <https://doi.org/10.3389/fmars.2022.850368>
- 404 Axenrot, T., Didrikas, T., Danielsson, C., & Hansson, S. (2004). Diel patterns in pelagic fish behaviour
 405 and distribution observed from a stationary, bottom-mounted, and upward-facing transducer. *ICES*
 406 *Journal of Marine Science*, *61*(7), 1100–1104. <https://doi.org/10.1016/j.icesjms.2004.07.006>
- 407 Baeten, N. J., Forwick, M., Vogt, C., & Vorren, T. O. (2010). Late Weichselian and Holocene
 408 sedimentary environments and glacial activity in Billefjorden, Svalbard. *Geological Society, London,*
 409 *Special Publications*, *344*(1), 207–223. <https://doi.org/10.1144/SP344.15>
- 410 Benoit, D., Simard, Y., & Fortier, L. (2008). Hydroacoustic detection of large winter aggregations of
 411 Arctic cod (*Boreogadus saida*) at depth in ice-covered Franklin Bay (Beaufort Sea). *Journal of*
 412 *Geophysical Research: Oceans*, *113*(C6), 2007JC004276. <https://doi.org/10.1029/2007JC004276>
- 413 Connolly, C. T., Cardenas, M. B., Burkart, G. A., Spencer, R. G. M., & McClelland, J. W. (2020).
 414 Groundwater as a major source of dissolved organic matter to Arctic coastal waters. *Nature*
 415 *Communications*, *11*(1), Article 1. <https://doi.org/10.1038/s41467-020-15250-8>
- 416 Deregibus, D., Campana, G. L., Neder, C., Barnes, D. K. A., Zacher, K., Piscicelli, J. M., Jerosch, K., &
 417 Quartino, M. L. (2023). Potential macroalgal expansion and blue carbon gains with northern Antarctic
 418 Peninsula glacial retreat. *Marine Environmental Research*, *189*, 106056.
 419 <https://doi.org/10.1016/j.marenvres.2023.106056>
- 420 Dunn, M., Pedersen, G., Basedow, S. L., Daase, M., Falk-Petersen, S., Bachelot, L., Camus, L., &
 421 Geoffroy, M. (2023). Inverse method applied to autonomous broadband hydroacoustic survey
 422 detects higher densities of zooplankton in near-surface aggregations than vessel-based net survey.
 423 *Canadian Journal of Fisheries and Aquatic Sciences*, *80*(3), 451–467. [https://doi.org/10.1139/cjfas-](https://doi.org/10.1139/cjfas-2022-0105)
 424 [2022-0105](https://doi.org/10.1139/cjfas-2022-0105)
- 425 Düsedau, L., Fredriksen, S., Brand, M., Fischer, P., Karsten, U., Bischof, K., Savoie, A., & Bartsch, I.
 426 (2024). Kelp forest community structure and demography in Kongsfjorden (Svalbard) across 25 years
 427 of Arctic warming. *Ecology and Evolution*, *14*(6), e11606. <https://doi.org/10.1002/ece3.11606>
- 428 Geoffroy, M., Cottier, F., Berge, J., & Inall, M. (2016). AUV-based acoustic observations of the
 429 distribution and patchiness of pelagic scattering layers during midnight sun. *ICES Journal of Marine*
 430 *Science*, *74*. <https://doi.org/10.1093/icesjms/fsw158>
- 431 Geoffroy, M., Daase, M., Cusa, M., Darnis, G., Graeve, M., Santana Hernández, N., Berge, J., Renaud,
 432 P. E., Cottier, F., & Falk-Petersen, S. (2019). Mesopelagic Sound Scattering Layers of the High Arctic:

- 433 Seasonal Variations in Biomass, Species Assemblage, and Trophic Relationships. *Frontiers in Marine*
434 *Science*, 6, 364. <https://doi.org/10.3389/fmars.2019.00364>
- 435 Gonzalez Trigriner, V., Beck, M., Sen, A., Bischof, K., & Damsgård, B. (2024). Acoustic mapping reveals
436 macroalgal settlement following a retreating glacier front in the High Arctic. *Frontiers in Marine*
437 *Science*, 11, 1438332. <https://doi.org/10.3389/fmars.2024.1438332>
- 438 Halbach, L., Vihtakari, M., Duarte, P., Everett, A., Granskog, M. A., Hop, H., Kauko, H. M., Kristiansen,
439 S., Myhre, P. I., Pavlov, A. K., Pramanik, A., Tatarek, A., Torsvik, T., Wiktor, J. M., Wold, A., Wulff, A.,
440 Steen, H., & Assmy, P. (2019). Tidewater Glaciers and Bedrock Characteristics Control the
441 Phytoplankton Growth Environment in a Fjord in the Arctic. *Frontiers in Marine Science*, 6.
442 <https://doi.org/10.3389/fmars.2019.00254>
- 443 Holmes, R. M., McClelland, J. W., Raymond, P. A., Frazer, B. B., Peterson, B. J., & Stieglitz, M. (2008).
444 Lability of DOC transported by Alaskan rivers to the Arctic Ocean. *Geophysical Research Letters*,
445 35(3). <https://doi.org/10.1029/2007GL032837>
- 446 Hop, H., Wold, A., Vihtakari, M., Assmy, P., Kuklinski, P., Kwasniewski, S., Griffith, G. P., Pavlova, O.,
447 Duarte, P., & Steen, H. (2023). Tidewater glaciers as “climate refugia” for zooplankton-dependent
448 food web in Kongsfjorden, Svalbard. *Frontiers in Marine Science*, 10.
449 <https://www.frontiersin.org/articles/10.3389/fmars.2023.1161912>
- 450 Hopwood, M. J., Carroll, D., Dunse, T., Hodson, A., Holding, J. M., Iriarte, J. L., Ribeiro, S., Achterberg,
451 E. P., Cantoni, C., Carlson, D. F., Chierici, M., Clarke, J. S., Cozzi, S., Fransson, A., Juul-Pedersen, T.,
452 Winding, M. H. S., & Meire, L. (2020). Review article: How does glacier discharge affect marine
453 biogeochemistry and primary production in the Arctic? *The Cryosphere*, 14(4), 1347–1383.
454 <https://doi.org/10.5194/tc-14-1347-2020>
- 455 James, N. C., & Whitfield, A. K. (2023). The role of macroalgae as nursery areas for fish species within
456 coastal seascapes. *Cambridge Prisms: Coastal Futures*, 1, e3. <https://doi.org/10.1017/cft.2022.3>
- 457 Kaartvedt, S., Røstad, A., Klevjer, T. A., & Staby, A. (2009). Use of bottom-mounted echo sounders in
458 exploring behavior of mesopelagic fishes. *Marine Ecology Progress Series*, 395, 109–118.
459 <https://doi.org/10.3354/meps08174>
- 460 Kavan, J., Luláková, P., Małecki, J., & Strzelecki, M. C. (2023). Capturing the transition from marine to
461 land-terminating glacier from the 126-year retreat history of Nordenskiöldbreen, Svalbard. *Journal of*
462 *Glaciology*, 1–11. <https://doi.org/10.1017/jog.2023.92>
- 463 Krause-Jensen, D., & Duarte, C. M. (2014). Expansion of vegetated coastal ecosystems in the future
464 Arctic. *Frontiers in Marine Science*, 1. <https://doi.org/10.3389/fmars.2014.00077>
- 465 Kruss, A., Tęgowski, J., Tatarek, A., Wiktor, J., & Blondel, P. (2017). Spatial distribution of macroalgae
466 along the shores of Kongsfjorden (West Spitsbergen) using acoustic imaging. *Polish Polar Research*,
467 38(2), 205–229. <https://doi.org/10.1515/popore-2017-0009>
- 468 Láska, K., Witoszová, D., & Prošek, P. (2012). Weather patterns of the coastal zone of Petuniabukta,
469 central Spitsbergen in the period 2008–2010. *Polish Polar Research*, 33(4), 297–318.
470 <https://doi.org/10.2478/v10183-012-0025-0>
- 471 Lippert, H., Iken, K., Rachor, E., & Wiencke, C. (2001). Macrofauna associated with macroalgae in the
472 Kongsfjord (Spitsbergen). *Polar Biology*, 24(7), 512–522. <https://doi.org/10.1007/s003000100250>

- 473 Lydersen, C., Assmy, P., Falk-Petersen, S., Kohler, J., Kovacs, K. M., Reigstad, M., Steen, H., Strøm, H.,
 474 Sundfjord, A., Varpe, Ø., Walczowski, W., Weslawski, J. M., & Zajaczkowski, M. (2014). The
 475 importance of tidewater glaciers for marine mammals and seabirds in Svalbard, Norway. *Journal of*
 476 *Marine Systems*, 129, 452–471. <https://doi.org/10.1016/j.jmarsys.2013.09.006>
- 477 Nilsen, F., Cottier, F., Skogseth, R., & Mattsson, S. (2008). Fjord–shelf exchanges controlled by ice and
 478 brine production: The interannual variation of Atlantic Water in Isfjorden, Svalbard. *Continental Shelf*
 479 *Research*, 28(14), 1838–1853. <https://doi.org/10.1016/j.csr.2008.04.015>
- 480 Nowak, A., Hodgkins, R., Nikulina, A., Osuch, M., Wawrzyniak, T., Kavan, J., Łepkowska, E., Majerska,
 481 M., Romashova, K., Vasilevich, I., Sobota, I., & Rachlewicz, G. (2021). *From land to fjords: The review*
 482 *of Svalbard hydrology from 1970 to 2019 (SvalHydro)*. Svalbard Integrated Arctic Earth Observing
 483 System. <https://doi.org/10.5281/zenodo.4294063>
- 484 Osgood, G. J., McCord, M. E., & Baum, J. K. (2019). Using baited remote underwater videos (BRUVs)
 485 to characterize chondrichthyan communities in a global biodiversity hotspot. *PLOS ONE*, 14(12),
 486 e0225859. <https://doi.org/10.1371/journal.pone.0225859>
- 487 R Core Team. (2021). *R: A Language and Environment for Statistical Computing*. R Foundation for
 488 Statistical Computing. <https://www.R-project.org/>
- 489 Renaud, P. E., Berge, J., Varpe, Ø., Lønne, O. J., Nahrgang, J., Ottesen, C., & Hallanger, I. (2012). Is the
 490 poleward expansion by Atlantic cod and haddock threatening native polar cod, *Boreogadus saida*?
 491 *Polar Biology*, 35(3), 401–412. <https://doi.org/10.1007/s00300-011-1085-z>
- 492 Simmonds, E. J., & MacLennan, D. N. (2005). *Fisheries acoustics: Theory and practice* (2nd ed).
 493 Blackwell Science.
- 494 Stanton, T. K., Chu, D., & Wiebe, P. H. (1996). Acoustic scattering characteristics of several
 495 zooplankton groups. *ICES Journal of Marine Science*, 53(2), 289–295.
 496 <https://doi.org/10.1006/jmsc.1996.0037>
- 497 Szczuciński, W., Zajaczkowski, M., & Scholten, J. (2009). Sediment accumulation rates in subpolar
 498 fjords – Impact of post-Little Ice Age glaciers retreat, Billefjorden, Svalbard. *Estuarine, Coastal and*
 499 *Shelf Science*, 85(3), 345–356. <https://doi.org/10.1016/j.ecss.2009.08.021>
- 500 Teagle, H., Hawkins, S. J., Moore, P. J., & Smale, D. A. (2017). The role of kelp species as biogenic
 501 habitat formers in coastal marine ecosystems. *Journal of Experimental Marine Biology and Ecology*,
 502 492, 81–98. <https://doi.org/10.1016/j.jembe.2017.01.017>
- 503 Terhaar, J., Lauerwald, R., Regnier, P., Gruber, N., & Bopp, L. (2021). Around one third of current
 504 Arctic Ocean primary production sustained by rivers and coastal erosion. *Nature Communications*,
 505 12(1), 169. <https://doi.org/10.1038/s41467-020-20470-z>
- 506 Urmy, S. S., Horne, J. K., & Barbee, D. H. (2012). Measuring the vertical distributional variability of
 507 pelagic fauna in Monterey Bay. *ICES Journal of Marine Science*, 69(2), 184–196.
 508 <https://doi.org/10.1093/icesjms/fsr205>
- 509 Varpe, Ø., & Gabrielsen, G. W. (2022). Aggregations of foraging black guillemots (*Cephus*
 510 *grylle*) at a sea-ice edge in front of a tidewater glacier. *Polar Research*, 41.
 511 <https://doi.org/10.33265/polar.v41.7141>
- 512 Vonnahme, T. R., Persson, E., Dietrich, U., Hejdukova, E., Dybwad, C., Elster, J., Chierici, M., &
 513 Gradinger, R. (2021). Early spring subglacial discharge plumes fuel under-ice primary production at a

514 Svalbard tidewater glacier. *The Cryosphere*, 15(4), 2083–2107. [https://doi.org/10.5194/tc-15-2083-](https://doi.org/10.5194/tc-15-2083-2021)
515 2021

516 Wiktor, J. M., Tatarek, A., Kruss, A., Singh, R. K., Wiktor, J. M., & Søreide, J. E. (2022). Comparison of
517 macroalgae meadows in warm Atlantic versus cold Arctic regimes in the high-Arctic Svalbard.
518 *Frontiers in Marine Science*, 9, 1021675. <https://doi.org/10.3389/fmars.2022.1021675>

519 Włodarska-Kowalczyk, M., Kukliński, P., Ronowicz, M., Legeżyńska, J., & Gromisz, S. (2009). Assessing
520 species richness of macrofauna associated with macroalgae in Arctic kelp forests (Hornsund,
521 Svalbard). *Polar Biology*, 32(6), 897–905. <https://doi.org/10.1007/s00300-009-0590-9>

522

523 Tables

524 Table 1. Bottom depth (m) and descriptive statistics of the oceanographic measurements per station
525 and year. Temperature in degrees Celsius, salinity in practical salinity units and turbidity in
526 nephelometric turbidity units (ntu).

Station	Year	Bottom Temperature Salinity Turbidity			
		depth	range	range	range
RIV	2022	37.6	7.1	14.5	13.1
RIV	2023	34	6.5	9.2	8.4
GLA	2022	46.4	7.6	18.2	102.5
GLA	2023	50.6	9.5	11.7	22.7
CON	2022	53.7	10	8.1	2.5
CON	2023	54.4	9.8	3.8	2.8

527

528 Table 2. Results from the integration of the acoustic data showing Sv mean, center of mass, inertia
529 and standard deviation for the means of all the replicates.

Station	Year	Bottom depth Sv mean Center of Inertia Standard				
		range (m)	(m ² /m ³)	mass (m)	(m ²)	deviation
RIV	2022	24 - 42	5.3e-09	13.2	66.4	1.7e-07

RIV	2023	24 - 43	1.6e-07	24.8	102.6	8.5e-06
GLA	2022	10 - 49	7.6e-09	24.7	147.2	1.5e-07
GLA	2023	5 - 56	3.3e-08	22.4	169.7	1.2e-06
CON	2022	7 - 45	8.9e-07	17.1	44.9	2.7e-05
CON	2023	13 - 50	2.2e-07	31.3	97.3	6.3e-06

530

531 Table 3. PERMANOVA with 999 permutations of Sv mean as the response variable and temperature,
532 turbidity, depth bin, year and station as explanatory variables.

	Df	SumOfSqs	R2	F	Pr(>F)
Temperature	1	0.86	0.01	4.87	0.005
Turbidity	1	4.93	0.08	27.89	0.001
Year	1	10.57	0.17	59.74	0.001
Station	2	6.18	0.10	17.48	0.001
DepthBin	1	1.27	0.02	7.16	0.001
Residual	226	39.97	0.63	NA	NA
Total	232	63.79	1.00	NA	NA

533

534 Table 4. PERMANOVA with 999 permutations of Sv mean as the response variable and salinity,
535 turbidity, depth bin, year and station as explanatory variables.

	Df	SumOfSqs	R2	F	Pr(>F)
Salinity	1	0.25	0.00	1.40	0.236
Turbidity	1	4.91	0.08	27.55	0.001
Year	1	11.05	0.17	62.05	0.001
Station	2	6.34	0.10	17.79	0.001

DepthBin	1	0.97	0.02	5.47	0.003
Residual	226	40.26	0.63	NA	NA
Total	232	63.79	1.00	NA	NA

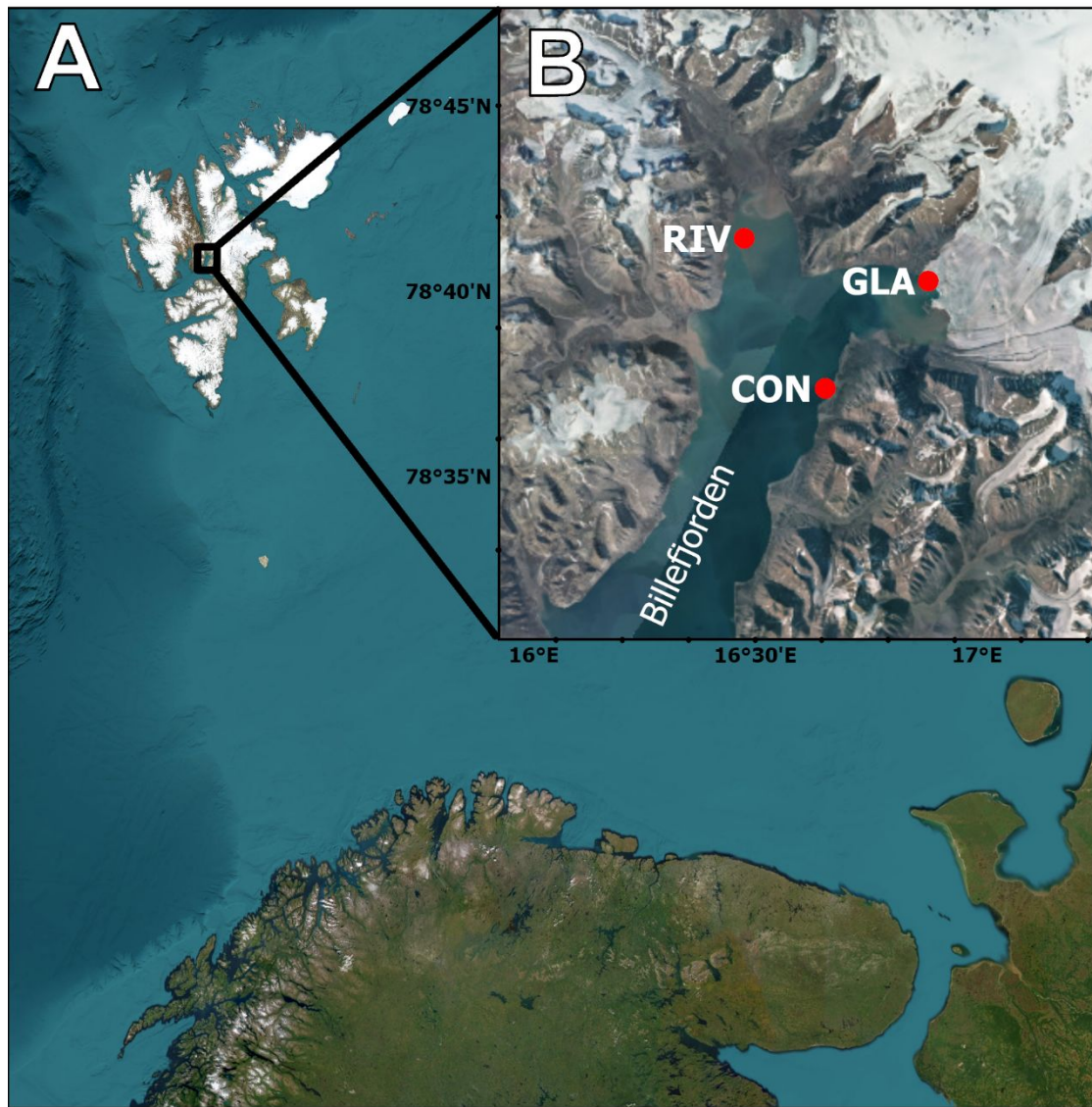
536

537 Table 5. Summary of the BRUV deployment data and maximum observed number of a taxa in a single
 538 frame (MaxN). There were 60 observations per hour (1 minute each) at every station, and all
 539 deployments were done at 10 m depth.

Station	Latitude (°N)	Longitude (°E)	Fish MaxN	Zooplankton MaxN
CON	78°37.063	16°40.704	6	100+
GLA	78°40.062	16°55.563	3	0
RIV	78°41.054	16°27.768	0	0

540

541 **Figures**

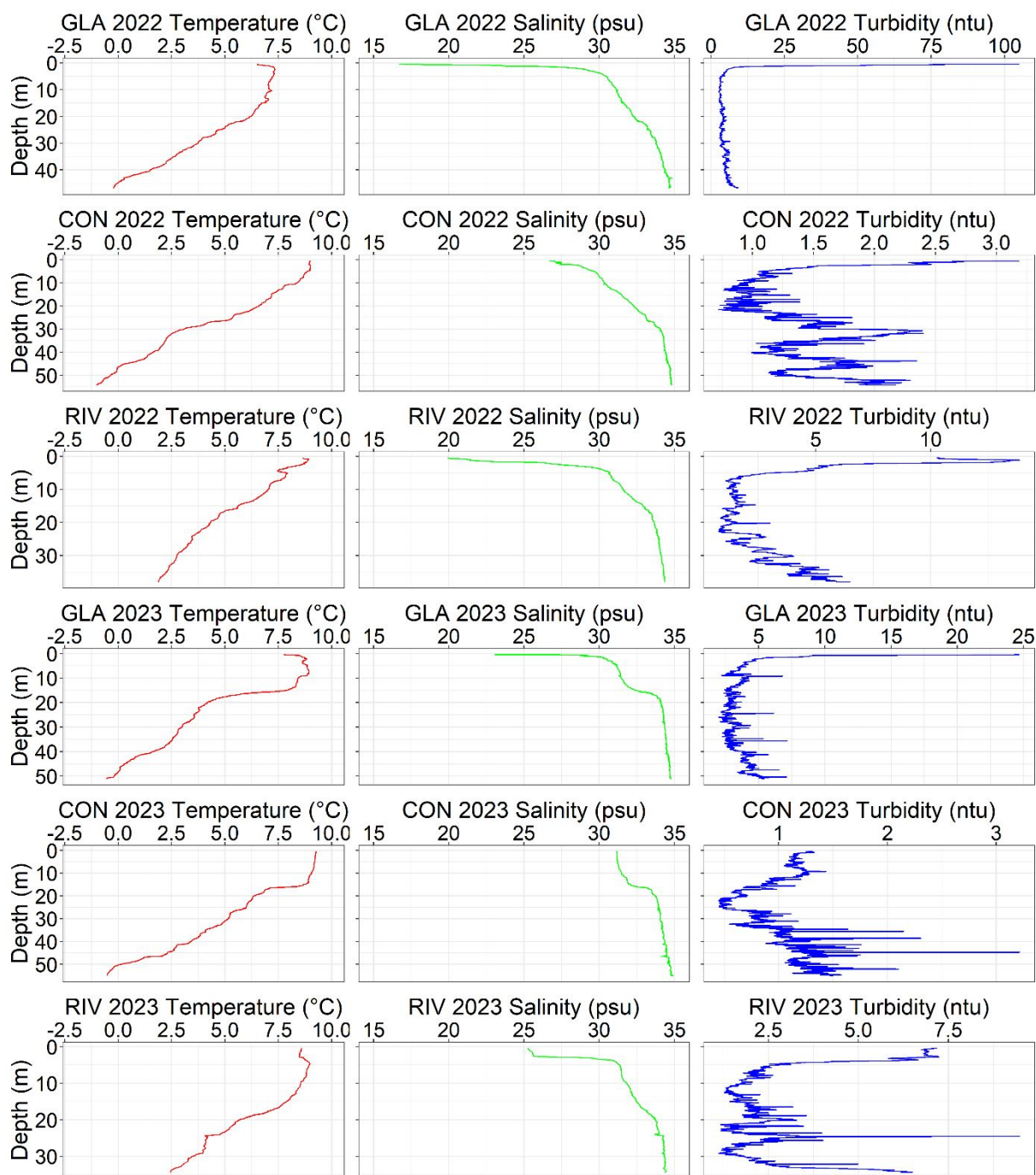


542

543 Figure 1. A) Study area in Svalbard. B) Satellite image of Billefjorden with the study stations (site with

544 a recently land-terminating glacier – GLA, river bay – RIV and site with low glacial input - CON. Map

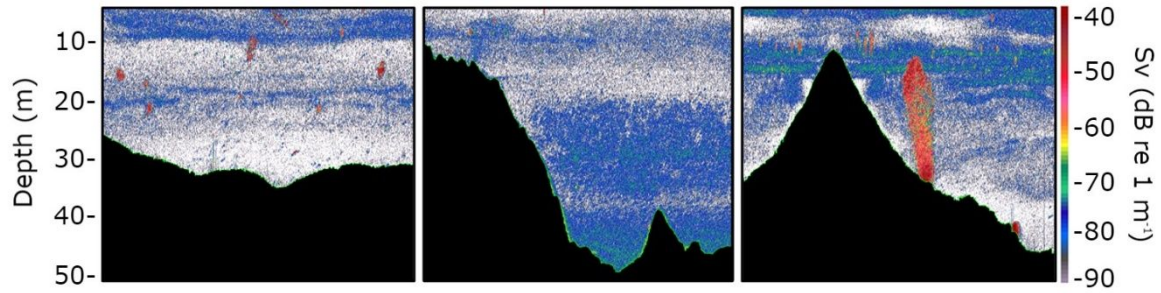
545 source: Earthstar Geographics and Norwegian Polar Institute.



546

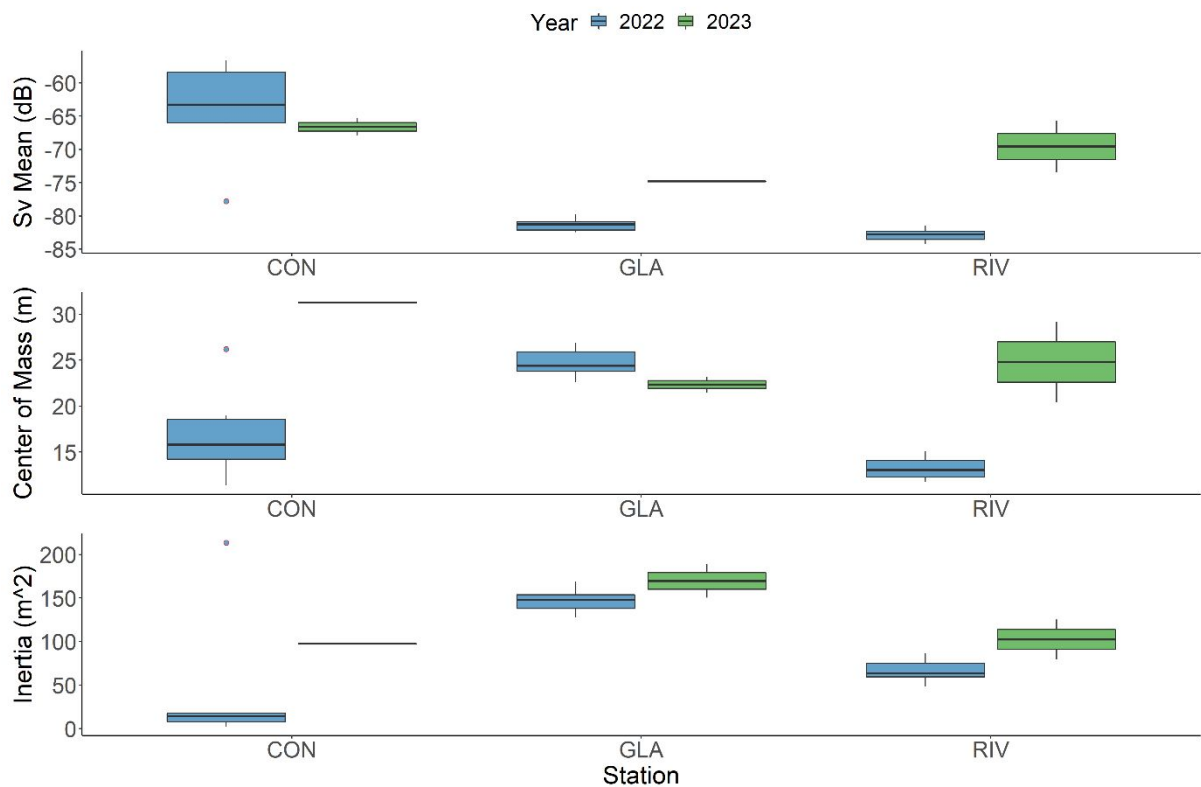
547 Figure 2. CTD water column profiles for the glacier (GLA), CON and river station (RIV) in 2022 and

548 2023 with measurements of temperature, salinity and turbidity.



549

550 Figure 3. Echogram snapshots of the RIV (left), GLA (middle) and CON (right) stations from 2023.



551

552 Figure 4. Differences among stations in acoustic parameters (logarithmic Sv mean, center of mass and

553 inertia). Mean values for Sv, center of mass and inertia were extracted for each transect (6 replicates

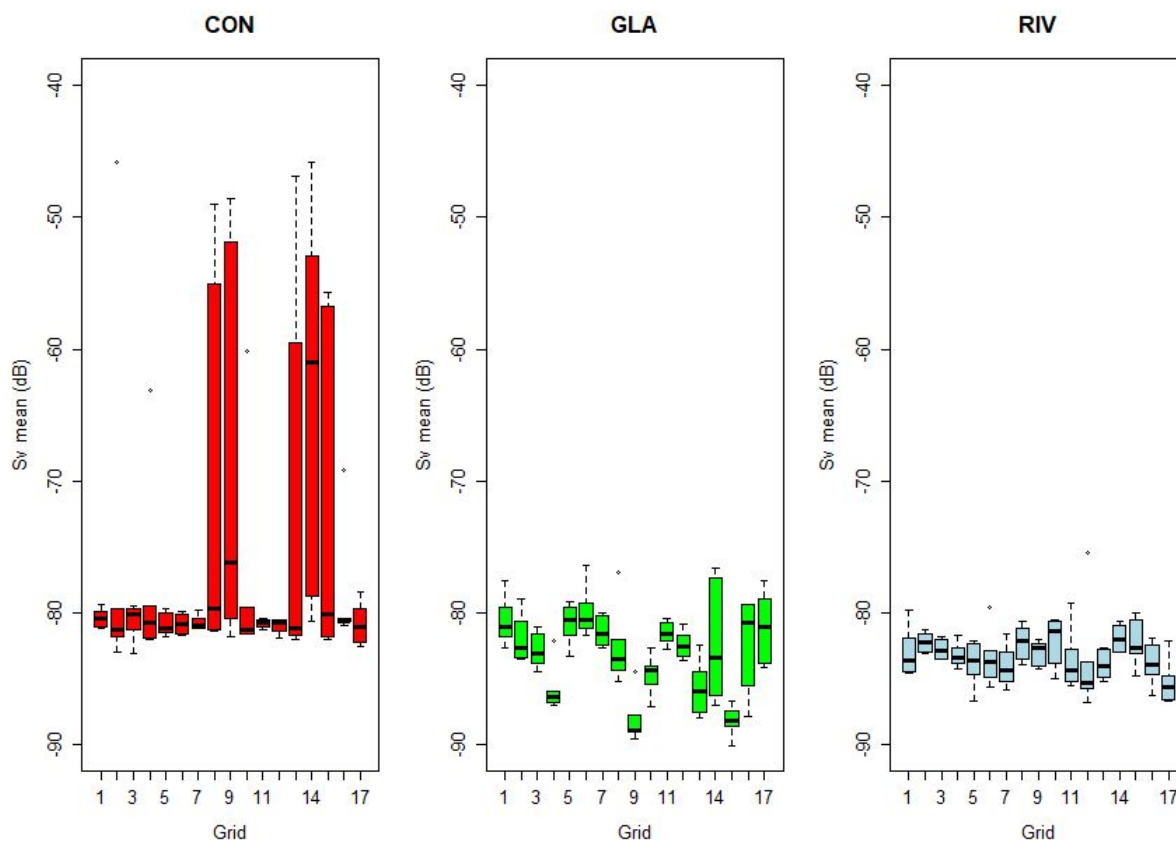
554 in 2022 and 2 replicates in 2023) and are presented by station and year. The box represents the

555 interquartile range (IQR) and the line within indicates the median. The whiskers extend to the most

556 extreme data points not considered outliers, which are represented by individual dots beyond the

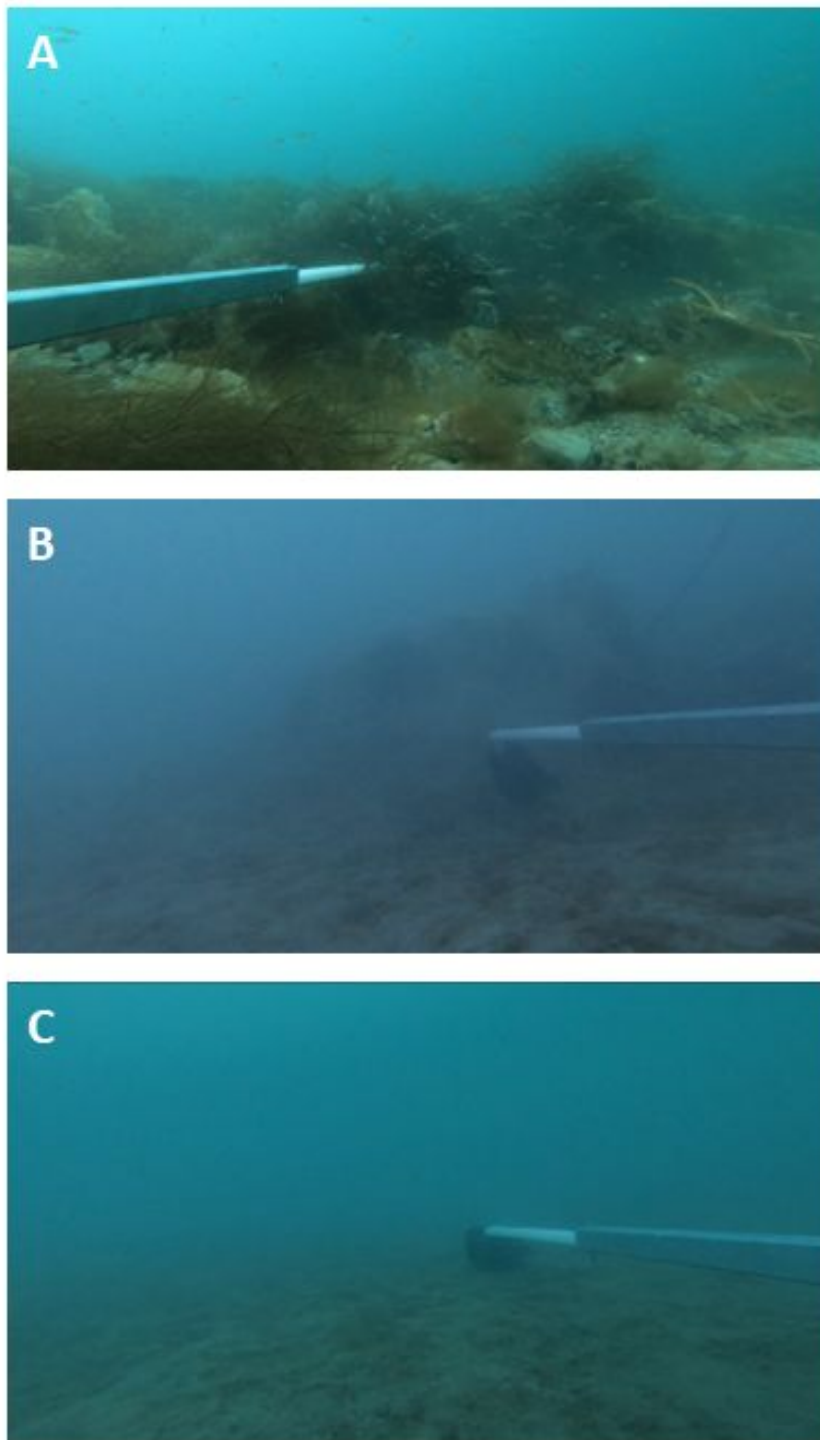
557 whiskers.

558



559
 560 Figure 5. Boxplots showing the ranges of Sv (dB) mean for each grid at the CON, GLA and RIV stations
 561 in 2022.

562



563

564

565 Figure 6. Snapshots from the BRUV deployment at (A) the CON station, (B) the GLA station and (C)

566 the RIV station.

567

568